JOURNAL OF MAGNETIC RESONANCE **134,** 36–43 (1998)
ARTICLE NO. MN981482

A Rectangular Loop–Gap Resonator for EPR Studies of Aqueous Samples

Wojciech Piasecki,* Wojciech Froncisz,*,[1] and Wayne L. Hubbell†

*Department of Biophysics, Institute of Molecular Biology, Jagiellonian University, Al. Mickiewicza 3, 31-120 Kraków, Poland; and
†Jules Stein Eye Institute and Department of Chemistry and Biochemistry, University of California, Los Angeles, Los Angeles, California 90024

Received February 4, 1998

A new rectangular geometry of the loop–gap resonator for the use with a flat cell has been developed. Maxwell's equations for the resonators with two, four, six, and eight gaps have been solved assuming the existence of only the magnetic *z*-component. The formulas obtained were numerically solved for the electric and magnetic field distributions over the cross-sections of the resonators. The presence of a nodal plane for the electric field in the center of the resonator allows the use of a flat cell instead of a capillary for EPR measurements. Using the field distributions obtained, the quality factor and EPR signal amplitude for various shapes and gap numbers for the resonators containing a flat cell filled with water were examined numerically. This allowed finding the geometry that yields the maximum EPR signal intensity. Several X-band resonators were built in order to verify the results obtained theoretically. The experiments confirmed the ability of a novel resonant structure to accommodate a flat cell filled with an aqueous sample. It has been found that the optimum aqueous sample volume for the X-band rectangular loop–gap resonator equals 16 mm^3. For a saturable aqueous sample this gives a fourfold improvement in the *S*/*N* ratio over the circular 1 mm i.d. loop–gap resonator equipped with 0.6 mm i.d. capillary. © 1998 Academic Press

INTRODUCTION

The concept of a loop–gap resonator (LGR), developed for EPR spectroscopy, is based on a lumped circuit (*1*). The properties of the circular loop–gap resonators has been thoroughly studied (*1–3*). Basic parameters of the resonators, i.e., resonant frequency *f,* quality factor *Q*, filling factor η, and efficiency parameter λ were calculated. The approach used in these early studies, however, did not allow calculating EPR sensitivity of the loop–gap resonator for aqueous samples, which are predominant in most biological studies. The first accurate calculations of the field distributions were performed for the so-called bridged loop–gap resonator (*4*). An analysis of field distributions in circular multigap loop–gap resonators was presented in our previous article (*5*). Using the field distributions, the quality factor and signal amplitude for the resonator containing a capillary filled with water were calculated numerically.

In this paper we present a novel loop–gap resonator with a rectangular central loop. To our knowledge this is a second attempt to find an alternative to the rectangular TE_{102} or cylindrical TM_{110} cavities commonly used in EPR spectroscopy to study aqueous samples. In the first attempt, a three-loop two-gap geometry was proposed (*6*). In that structure a central loop had a circular shape. Optimum performance with the resonator was achieved for 1 mm flat cells filled with approximately 100 mm^3 of a saturable aqueous sample. Under these conditions, a *S*/*N* ratio similar to the rectangular cavity with the active sample volume of 50 mm^3 was achieved. This rather poor sensitivity was due to its low microwave efficiency factor, $\lambda = 0.85$, which for the TE_{102} cavity is $\lambda = 1.17$ (*7*). That is, the product of the quality factor, *Q*, and filling factor, η, proportional to the EPR signal intensity (*8*, *9*), was similar for the two structures.

In the new rectangular loop–gap resonator, the optimum performance for aqueous samples was achieved for a six-gap structure. This gives an EPR signal amplitude comparable to the TE_{102} cavity with a sample volume of only 16 mm^3. Additionally, its low value *Q* factor is desirable to obtain a short ringing time in pulse EPR spectroscopy. Low *Q* resonators are also essential in CW ELDOR, CW dispersion EPR, and multiquantum EPR experiments.

THEORY

Field Distributions

Four rectangular loop–gap resonators with different numbers of gaps were studied. Their cross-sectional views are presented in Fig. 1.

The approach used to find field distributions over the cross-sections of the examined structures is similar to that described in our previous article, in which circular LG resonators were examined (*5*).

[1] To whom correspondence should be addressed.

1090-7807/98 $25.00
Copyright © 1998 by Academic Press
All rights of reproduction in any form reserved.

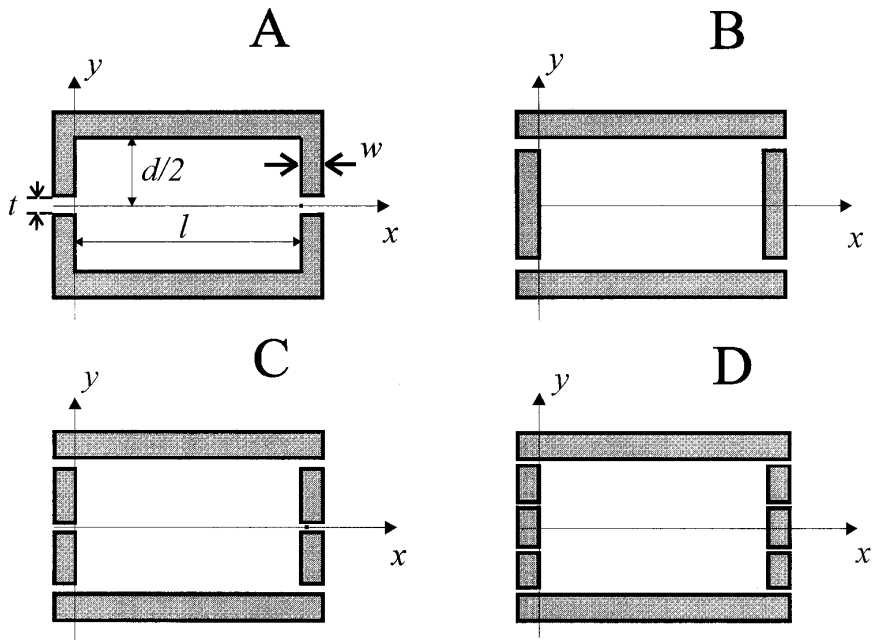

FIG. 1. Cross-sectional views of two-, four-, six-, and eight-gap rectangular resonators (A, B, C, and D, respectively).

In order to solve Maxwell's equations, proper boundary conditions must be defined. For the structures in Fig. 1, the *y*-component of the electric field has a constant value in the gaps (E at $x = 0$ and $-E$ at $x = l$). Outside the gaps at $x = 0$ and $x = l$ the *y*-component of the electric field is zero. Solving Maxwell's equations with the assumption that the resonators are sufficiently long is straightforward and is presented step-by-step by Kroll (*10*) and by Piasecki and Froncisz (*5*). The assumption of a long resonator implies no variation of field components along the *z*-axis and that the E_z component of the electric field equals zero. Thus, only E_x, E_y, and H_z are to be found. The solutions to Maxwell's equations are as follows:

$$E_x = -\frac{4E}{d}\sum_{p=1}^{\infty}\frac{1}{k_x}\Gamma(p,t,d)\left(\frac{1+e^{k_x l}}{e^{k_x l}-e^{-k_x l}}e^{-k_x x} + \frac{1+e^{-k_x l}}{e^{k_x l}-e^{-k_x l}}e^{k_x x}\right)\sin\left(\frac{2p\pi}{d}y\right) \quad [1]$$

$$E_y = E\left\{\frac{2}{\pi}\left[\sum_{p=1}^{\infty}\frac{1}{p}\Gamma(p,t,d)\left(\frac{1+e^{k_x l}}{e^{k_x l}-e^{-k_x l}}e^{-k_x l} + \frac{1+e^{-k_x l}}{e^{k_x l}-e^{-k_x l}}e^{k_x x}\right)\cos\left(\frac{2p\pi}{d}y\right)\right] + \frac{t}{d}\frac{\sin(k(l-x))-\sin(kx)}{\sin(kl)}\right\} \quad [2]$$

$$H_z = jE\sqrt{\frac{\varepsilon_0}{\mu_0}}\left\{\frac{2k}{\pi}\left[\sum_{p=1}^{\infty}\frac{1}{pk_x}\Gamma(p,t,d) \times\left(\frac{1+e^{k_x l}}{e^{k_x l}-e^{-k_x l}}e^{-k_x x} + \frac{1+e^{-k_x l}}{e^{k_x l}-e^{-k_x l}}e^{k_x x}\right)\cos\left(\frac{2p\pi}{d}y\right)\right] - \frac{t}{d}\frac{\cos(kx)+\cos(k(l-x))}{\sin(kl)}\right\}. \quad [3]$$

The quantity $\Gamma(p, t, d)$ depends on the boundary conditions and for the four resonators examined is given by

$$\Gamma(p,t,d) = \sin\left(\frac{pt\pi}{d}\right) \text{ for resonator A} \quad [4]$$

$$\Gamma(p,t,d) = \sin\frac{p\pi(2t-d)}{d} \quad \text{for resonator B} \quad [5]$$

$$\Gamma(p,t,d) = \sin\frac{p\pi 3t}{3d} + \sin\frac{p\pi(6t-3d)}{3d} \quad \text{for resonator C} \quad [6]$$

$$\Gamma(p,t,d) = \sin\frac{p\pi(4t-2d)}{2d} + \sin\frac{p\pi(4t-d)}{3d} + \sin\frac{p\pi(2d-4t)}{6d} \quad \text{for resonator D,} \quad [7]$$

where l and d are the resonator length and width, respectively, and t is the gap thickness as shown in Fig. 1.

Resonant Frequency

To a first approximation, a loop–gap resonator can be treated as a lumped circuit in which the ''loop'' is simply an inductance and the ''gap'' is a capacitor. This makes the loop–gap resonator a very flexible structure for which, in contrast to a classical resonant cavity, the resonant frequency and the inner dimensions are not linked directly. The lumped circuit approximation, however, implies that the dimensions of the resonator are much smaller than the wavelength. With the above assumptions, a rectangular loop–gap resonator is composed of an inductance formed by a rectangular cylinder of height h and a series of parallel capacitors formed by parallel rectangular plates of dimensions $h \times w$ separated by t. Thus, the resonant frequency can be expressed as

$$f = \frac{1}{2\pi\sqrt{LC}}, \qquad [7]$$

where

$$L = \frac{2\mu_0}{\pi h}\, ld\left(\arctan\frac{2l\sqrt{\left(\frac{h}{2}\right)^2+\left(\frac{l}{2}\right)^2+\left(\frac{d}{2}\right)^2}}{hd} + \arctan\frac{2d\sqrt{\left(\frac{h}{2}\right)^2+\left(\frac{l}{2}\right)^2+\left(\frac{d}{2}\right)^2}}{hl}\right) \qquad [8]$$

is the inductance of the center loop. Equation [8] was derived with the assumption that the center loop is a long rectangular cylinder of thin walls with a thickness equal to a few skin depths (the skin depths for microwave frequencies are on the order of micrometers). The capacitance C represents a series of parallel plate capacitors. Thus,

$$C = \frac{\varepsilon_0 hw}{nt}, \qquad [9]$$

where w is the gap width and n is the number of gaps. From the expressions above it can be seen that for the same dimensions of the rectangular loop one can obtain a wide spectrum of resonant frequencies by varying the gap width w or thickness t. At the same time, for a given resonant frequency, a resonator that gives maximum EPR signal intensity for a given sample geometry and dielectric properties can be easily designed.

Quality Factor and EPR Signal Amplitude

The quality factor of a resonator is defined by the formula (*8, 11*)

$$Q = \omega_0 \times \frac{W_s}{P_l}, \qquad [10]$$

where W_s is the energy stored in the resonator and P_l is the energy dissipated in one cycle. If it is assumed that the microwave electric field distribution in the resonator is not affected by the presence of the aqueous sample (*5, 8*), one can calculate the power dissipated in the sample due to the imaginary component of the dielectric constant. The ratio of the loaded quality factor for the resonator containing a lossy sample (Q_l) and the loaded Q for the same empty resonator (Q_e) is very useful for studying properties of the resonator in the sense of obtaining maximum filling factor (η) without significantly degrading the quality factor. For a critically coupled resonator containing water, the ratio takes the form (*5*)

$$\frac{Q_l}{Q_e} = \left\{1 + 2Q_e\frac{\varepsilon''\iiint_{V_S}|E(x,y)|^2dV}{\mu_0\iiint_{V_R}|H_z(x,y)|^2dV}\right\}^{-1}. \qquad [11]$$

In Eq. [11], V_R is the volume of the resonator and V_S is the volume of the sample. In deriving the equation it has been assumed that the value of Q_e is determined only by the finite conductivity of the resonator walls, and that the effect of degrading the quality factor is attributable only to the imaginary part of the dielectric constant (ε''). The EPR signal intensity, S, depends on the quality factor of the resonator and the filling factor η, defined as (*6, 7*)

$$\eta = \frac{\iiint_{V_S}H_z^2dV_S}{\iiint_{V_R}H_z^2dV_R}. \qquad [12]$$

S can then be expressed as

$$S = Cf_0Q\eta\sqrt{P_i}, \qquad [13]$$

where f_0 is the resonant frequency, P_i is the microwave incident power, and C is a constant dependent on the nature of the sample, temperature, and the parameters of the EPR spectrometer (the modulation amplitude and the noise figure, for example). Because of the dependence of S on the spectrometer characteristics, the absolute value of the EPR signal intensity is difficult to calculate. However, for the sake of comparing resonant structures, relative values of S, proportional to $Q\eta$, are very useful. Thus, the dependence of the product $Q\eta$ on the size and shape of the sample permits finding the sample geometry which yields maximum signal intensity. Alternatively, for a given sample geometry, the optimum geometry of the resonator can be found.

It must be noted that the microwave magnetic field amplitude inside a real resonator is reduced because the energy of the microwave field is stored not only in the central loop, but also in the side loops, which house the return magnetic flux (see

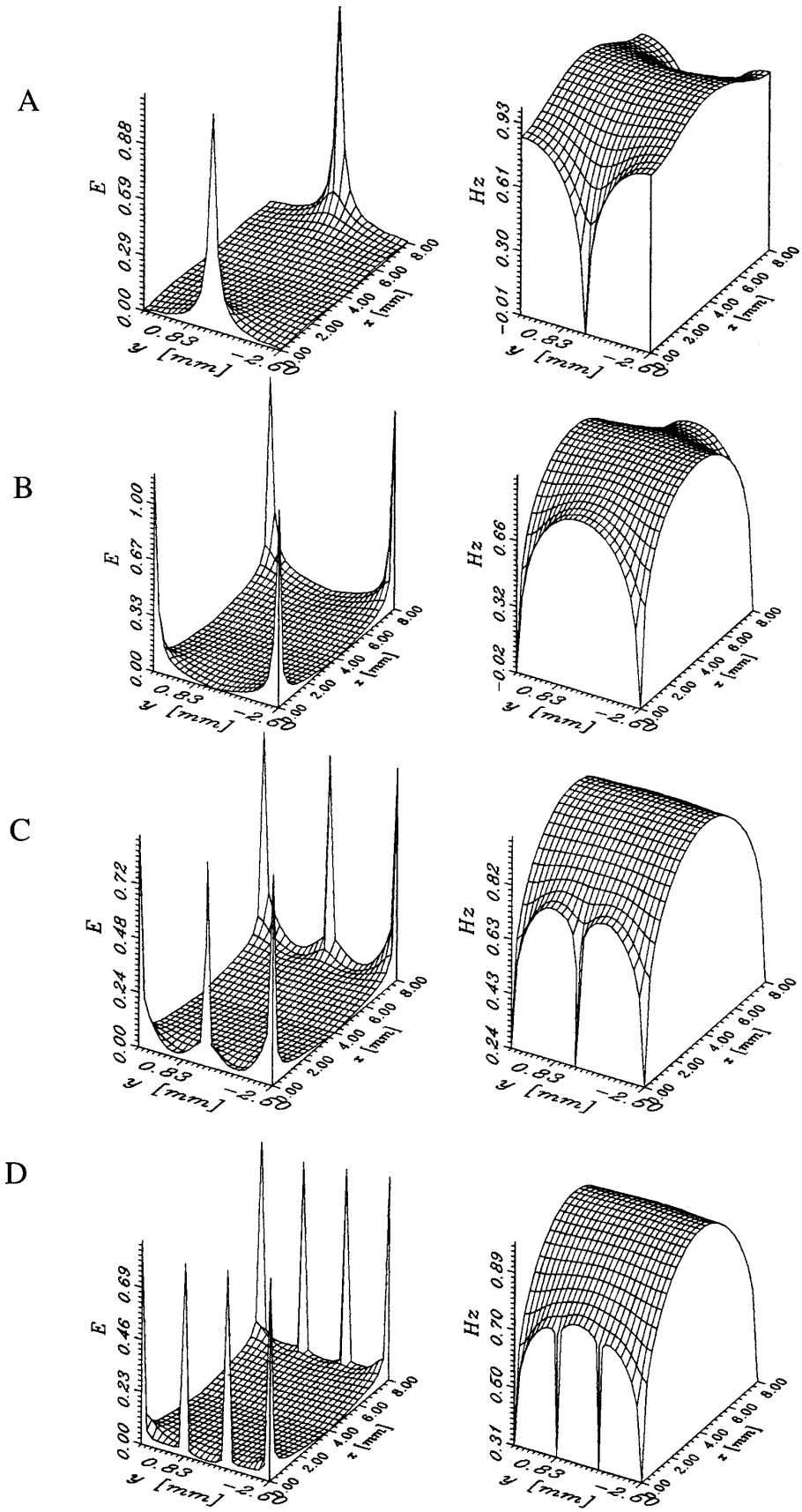

FIG. 2. Electric, E, and magnetic, H_z, field distribution over cross-section of the rectangular loop–gap resonators with two (A), four (B), six (C), and eight (D) gaps.

Fig. 3). Thus, the filling factor for a given sample and resonator with side loops is decreased, with respect to the ideal resonator with an infinite side-loop cross-section, by a factor of

$$\frac{S_{side}}{S_{center} + S_{side}}, \qquad [14]$$

where S_{center} and S_{side} are the areas of the cross-sections of the center loop and side loops, respectively.

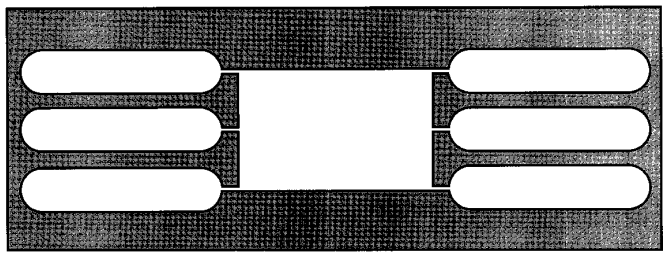

FIG. 3. Cross-sectional view of the test six-gap rectangular resonator.

RESULTS AND DISCUSSION

Field Distribution in Empty Resonators

In order to study the properties of the resonators, computer programs have been written that allow numerical calculation of the electromagnetic field components over the cross-sections of the resonators as well as the dependence of the signal intensity and quality factor on a given sample geometry. The programs have been written in the Turbo Pascal 6.0 programming language for IBM PC compatible computers.

The results of the calculations of field distributions for the analyzed resonators obtained at $f = 9.5$ GHz are presented in Fig. 2. The dimensions of the loop of the resonators are $d = 5$ mm and $l = 8$ mm. The Z coordinate indicates a given field intensity related to its maximum value. The electric field components, E_x and E_y, are shown jointly as $\sqrt{E_x^2 + E_y^2}$. From the plots it can be seen that there is a nodal plane of the electric field in each resonator examined. This implies that the new rectangular structure of a loop–gap resonator is suitable for examining aqueous samples in a flat cell rather than in a capillary.

Quality Factor and EPR Signal Intensity for Aqueous Samples

The field distributions obtained were used for calculating numerically the dependence of the quality factor and signal amplitude on the aqueous sample thickness for various sizes of resonators. A series of numerical calculations provided the optimum shape and size of the resonator in the sense of yielding the maximum EPR signal intensity. The calculations, however, neglected changes in the field distribution caused by the aqueous sample.

Numerical calculations were also performed in order to find the optimum length of the resonator, for a given resonator width. For the resonator with six gaps and $d = 5$ mm, it was found that at $f = 9.5$ GHz the optimum length, l, of the resonator is 8 mm. The calculations assumed no changes in the field caused by the aqueous sample.

In order to verify the results of the calculations, several aluminum test resonators were built. The dependence of their basic electrical parameters, the resonant frequency and quality factor, on the aqueous sample thickness has been measured. All measurements of the EPR signal intensity for the model aluminum resonators were performed with the use of a Bruker ESP 300E spectrometer applying low frequency magnetic field modulation (1.56 kHz). The concentration of nitroxide spin label (Tempocholine) in aqueous samples was 1 mM. The geometry of the test resonators is presented in Fig. 3. Three aluminum resonators with l equal to 8, 4, and 2.4 mm were built. In all cases the center loop width d was 5 mm. Additionally, for high modulation frequency, one resonator was made of silver-plated Macor ceramic and had a geometry identical to the 4 mm long aluminum resonator (Fig. 3). In this resonator the six side loops house the return magnetic flux.

The resonators were coupled to the microwave coaxial line with a loop located at the end of the line. The loop was situated beneath the side loops where the return magnetic field of the resonator is present. The position of the coupling loop was adjustable in order to obtain critical coupling. Values of the quality factor were calculated from the 3 dB bandwidth of the resonant curves.

The results of the calculations, according to Eq. [11], of the relative quality factor for the resonators 8 mm long are presented in Fig. 4A. Calculations were performed for all four geometries. Additionally, the influence of the side loops on the resonator C was taken into account. Experimental results obtained for the model 8 mm aluminum resonator, also presented in Fig. 4A, are in good agreement with the calculations. Similar calculations were performed for the 4 mm long resonators. The results of the calculations and the experimental results obtained for a silver plated Macor resonator are shown in Fig. 4B.

In this case, in contrast to the 8 mm resonator, the experimentally measured decrease in the quality factor is much smaller than the calculated one. This means that for shorter resonators the assumption that the electric field distribution in the resonator is unchanged in the presence of an aqueous sample is not valid. The electric field intensity in the sample is smaller than calculated, causing the energy loss in the sample to be decreased.

The results of calculations of the $Q\eta$ product, which represents the EPR signal intensity for constant incident power, are presented in Figs. 5A and 5B for 8 and 4 mm long resonators, respectively. The resonators with six rather than eight gaps were found to yield the maximum EPR signal intensity out of the structures examined. This is a rather unexpected result

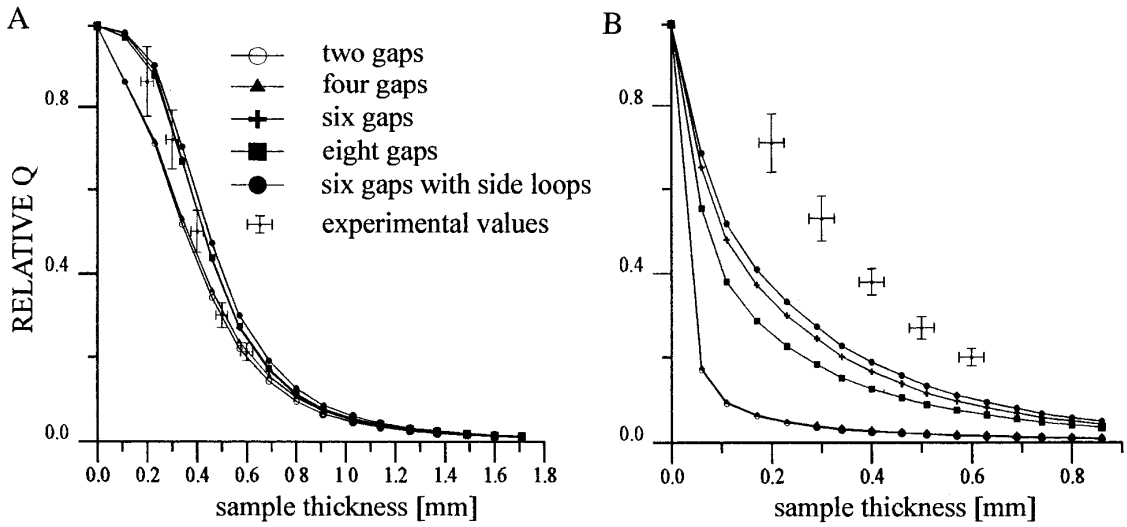

FIG. 4. Calculated dependence of the relative Q on the aqueous sample thickness for resonators with two, four, six, and eight gaps without side loops and six-gap resonator with side loops. All resonators were either 8 × 5 mm (A) or 4 × 5 mm (B) and the sample width was assumed to be 4 mm. Experimental results were obtained for an aluminum test resonator with six gaps and side loops.

because increasing the number of gaps might be expected to give better results in analogy with the circular loop–gap resonators (*5*). The better performance of the six-gap resonator is probably a result of two factors: the number of gaps and the symmetry of the electric field. In the series of resonators with $2 + 4n$ gaps, where $n = 0, 1, 2 \ldots$, there is an electric field in the center of the rectangular loop wall. Increasing the number of gaps decreases losses which are attributable to the presence of aqueous sample. Similarly, there is a monotonic dependence of losses on the number of gaps for $4 + 4n$ series. Changing the number of gaps from six to eight causes a change in the field symmetry, increasing losses in spite of the higher number of gaps.

Thus, it can be seen that in both cases analyzed (8 and 4 mm long resonators) the six gap resonator can accommodate the largest sample without significantly degrading its quality factor. For the 8 mm long resonator it was calculated that the maximum EPR signal intensity should be obtained for a sample 0.35 mm thick, which was confirmed by EPR measurements.

Thus, the 8 mm long resonator can accommodate an aqueous sample three times larger (in a flat cell of inner dimensions 0.35 × 4 mm) than a typical 5 mm diameter circular loop–gap resonator, which yields the maximum EPR signal when used with a capillary of 0.8 mm diameter (*5*).

The measured dependencies of the EPR signal amplitude on the sample thickness are in a good agreement with the calcu-

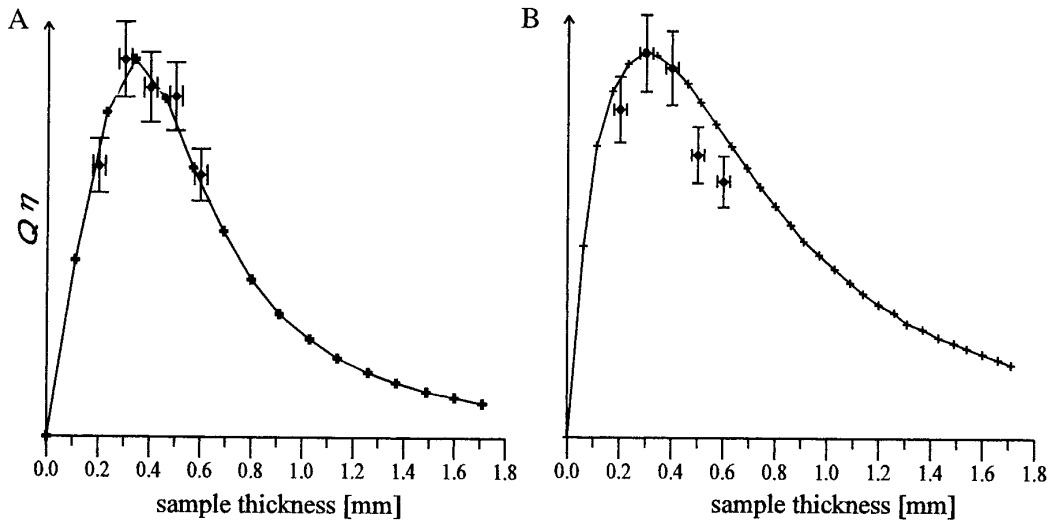

FIG. 5. Calculated (solid line) and experimental (crosses) dependence of the $Q\eta$ product, which represents the EPR signal intensity, on the sample thickness for resonators with six gaps. l equals 8 and 4 mm for A and B, respectively.

TABLE 1
Basic Parameters of Tested Resonators

Resonator	S_{center} [mm^2]	Q	f_0 [GHz]	EPR signal of DPPH at 1.5 mW	$\lambda\left[\frac{G}{\sqrt{W}}\right]$	Active volume of aqueous sample	ηQ	EPR signal of spin label (max. value)	EPR signal of spin label at 0.5 mW
5 × 8 mm aluminum, h = 1 cm	40	536	9.47	307	1.22	—	—	—	—
		314	9.44		—	0.4 × 4 × 10 mm flat cell (V_S = 16 mm^3)	11.8	649 at 100 mW	34
5 × 4 mm aluminum, h = 1 cm	18.7	635	9.22	680	1.81	—	—	—	—
		274	9.18		—	0.4 × 4 × 10 mm flat cell	20	863 at 100 mW	58
5 × 4 mm Macor, h = 1 cm	18.7	550	9.41	624	1.73	—	—	—	—
		220	9.37		—	0.4 × 4 × 10 mm flat cell	20	816 at 100 mW	58
5 × 2.4 mm aluminum, h = 1 cm	11	347	9.09	562	1.65	—	—	—	—
		207	9.02		—	0.4 × 4 × 10 mm flat cell	27.4	880 at 80 mW	85
Varian TE_{102} cavity	—	4070	9.51	284	1.17	— —	—	—	—
		2159	9.48		—	0.3 × 8.5 × 20 mm flat cell (V_S = 50 mm^3)	12	1269 at 200 mW	76
1 mm diameter LGR, h = 0.5 cm	0.81	393	9.22	8400	6.3	—	—	—	—
		162	9.16		—	0.63 mm ID capillary (V_S = 1.56 mm^3)	58.5	210 at 5 mW	118

lated ones. This means that, even though the calculations were simplified and neglected the changes in field distributions caused by the sample, the optimum thickness of the sample was, in both cases, evaluated correctly.

Comparative Measurements of the New Resonators

The parameters of the resonators tested and results of the basic measurements are listed in Table 1. Measurements with the use of a standard Varian TE_{102} cavity and a circular 1 mm diameter LGR were also performed in order to compare the new resonators with a traditional cavity and the commonly used, circular LGR. All the tested rectangular loop–gap resonators had six side loops and the geometry shown in Fig. 3. The second column in Table 1 specifies the area of the cross-section of the center loop of the loop–gap resonators tested. The third and fourth column give the measured quality factor and resonant frequency, respectively, for both empty and water-filled resonators. Even though calculations were performed with the assumption of a simple LC model, there is a good agreement between experimental and theoretical values (9.5 GHz) of the resonant frequency for all rectangular resonators. The calculations did not take into account the magnetic field present in the gaps, the electric field in the loop, and the magnetic fringe fields at the top and at the bottom of the resonator.

The fifth column gives information on the amplitude of a powder DPPH (2α-diphenyl-β-picrylhydrazil) point sample spectrum obtained at 1.5 mW of microwave power. The sixth column presents values of the efficiency parameter, λ, representing the peak microwave magnetic field intensities at the sample position for 1 W of incident power. The efficiency

parameter was calculated as the ratio of the DPPH signal amplitude recorded at the same incident microwave power for the resonator and for the standard Varian TE_{102} cavity, assuming that the λ value for this cavity equals 1.17 (*7*). During the measurements, the amplitude of the modulation was set so that the maximum signal amplitude was obtained. The ηQ product in the eighth column was calculated using the Q value from the third column, and a value of η calculated according to Eq. [12]. The ninth and tenth columns give the EPR signal intensities obtained for 0.35 mM Tempocholine spin label solution in water at the same amplitude of the modulation magnetic field. The ninth column is the maximum signal obtained when the microwave incident power is changed. Finally, the last column shows the EPR signal intensities for the same sample at 0.5 mW of microwave incident power. It can be seen from Table 1 that the simplified calculations of the EPR signal amplitude and quality factor, neglecting the sample influence on the field distributions, incorrectly predict the optimum length of the resonator. This is in contrast to the results obtained for circular loop–gap resonators (*5*).

The best resonator, in the sense of the maximum EPR signal or the efficiency parameter, is the 4 mm rather than the 8 mm one. This is because the electric field in the sample region is reduced significantly with respect to that of the empty resonator. The quality factor for the resonator loaded with the 0.4 mm thick sample is decreased only by a factor of 0.43, whereas the Q_l calculated for the 4 mm resonator with a 0.4 mm thick sample is only 0.167 of Q_e. The efficiency parameter λ equals 1.81, which means that 2.4 times less microwave incident power is required to achieve the same microwave magnetic field intensity, as in the Varian TE_{102} cavity.

CONCLUSIONS

It is apparent from our studies that the new rectangular resonator is superior to all proposed previously circular loop–gap resonators for aqueous samples. However, it is difficult to confirm whether the S/N ratio can be further improved for this class of samples by changing dimensions of that resonator. This is because the aqueous sample significantly modifies the field distribution when the resonator dimensions are small. In this case the solution of Maxwell's equations in the presence of an aqueous sample has to be found. This can be done, in principle, by using, for example, the Hewlett-Packard High Frequency Structure Simulator. However, computers using this program are not yet sufficiently fast to find an optimized design by automatically adjusting geometry to minimize a proper error function (*12*). Thus, the semiempirical approach presented in this paper seems to be justified at this moment.

ACKNOWLEDGMENTS

This work was supported by The Polish Committee for Scientific Research Grant P03B 100 09 and Fogarty International Research Collaboration No. 1 R03 TW00456-01.

REFERENCES

1. W. Froncisz and J. S. Hyde, *J. Magn. Reson.* **47,** 515 (1982).
2. M. Mehdizadeh, ''An Investigation on Electromagnetic Field and Properties of the Loop-Gap Resonator, a Lumped Mode Microwave Resonant Structure.'' Ph.D. Thesis, Marquette University, Milwaukee, WI (1983).
3. W. Froncisz, T. Oles, and J. S. Hyde, *Rev. Sci. Instrum.* **57,** 1095 (1986).
4. S. Pfenninger, J. Forrer, A. Schweiger, and Th. Weiland, *Rev. Sci. Instrum.* **59,** 752 (1988).
5. W. Piasecki and W. Froncisz, *Meas. Sci. Technol.* **4,** 1363 (1993).
6. J. S. Hyde, W. Froncisz, and T. Oles, *J. Magn. Reson.* **82,** 223 (1989).
7. R. D. Rataiczak and M. T. Jones, *J. Chem. Phys.* **56,** 3898 (1972).
8. P. Dalal, S. S. Eaton, and G. R. Eaton, *J. Magn. Reson.* **44,** 415 (1981).
9. G. Feher, *Bell System Tech. J.* **36,** 449 (1956).
10. N. Kroll, ''Microwave Magnetrons,'' pp. 49–61, McGraw–Hill, New York (1948).
11. G. Stoodley, *Electron. Control* **14,** 531 (1963).
12. W. Piasecki, W. Froncisz, and J. S. Hyde, *Rev. Sci. Instrum.* **67,** 1896 (1996).